Article

Journal of
Nanoscience and Nanotechnology
Vol. 14, 1–5, 2014
www.aspbs.com/jnn

Multifunctional Nanobiocomposite of Poly[(butylene succinate)-co-adipate] and Clay

Shaeel A. Al-Thabaiti[1], Suprakas Sinha Ray[1, 2, *],
Sulaiman Nassir Basahel[1], and Mohamed Mokhtar[1]

[1] *Department of Chemistry, King Abdulaziz University, Jeddah 21589, Kingdom of Saudi Arab*
[2] *DST/CSIR National Centre for Nanostructured Materials, Council for Scientific and Industrial Research, Pretoria 0001, South Africa*

The processing and characterization of multifunctional nanobiocomposite of biodegradable poly[(butylene succinate)-co-adipate] (PBSA) and organically modified synthetic fluorine mica (OSFM) are reported. The nanobiocomposite of PBSA with OSFM was prepared using melt-blending, and the structure and morphology of the nanocomposite were characterized using X-ray diffraction and transmission electron microscopy. The mechanical and material properties measurements showed the concurrent improvement in temperature dependence storage modulus, tensile properties, gas barrier, and thermal stability of neat PBSA after nanocomposite formation. Such improved inherent properties along with the environmentally-friendly feature are expected to widen the use of PBSA for short-term food-packaging applications.

Keywords: Poly[(butylenes succinate)-co-adipate], Organically Modified Synthetic Mica, Multi-Functional Properties.

1. INTRODUCTION

Over the last few years, the demand for environmentally-friendly polymeric materials with a balance of mechanical and material properties is said to be growing at a rapid rate. Environmentally-friendly or biodegradable polymers can be produced from biosources such as corn, wood cellulose, etc.[1–3] or can also be synthesized by bacteria from small molecules such as butyric acid or valeric acid, which yield poly(hydroxybutyrate) and polyhydroxyvalerate.[1, 2] In addition, biodegradable polymers can also be derived from the petroleum sources, such as poly(ε-caprolactone), poly(butylene succinate), poly[(butylene succinate)-co-adipate], poly(butylene adipate-co-terephthalate), or can be obtained from mixed sources of biomass and petroleum.[1, 2] The best-known petroleum source-derived biodegradable polymers are aliphatic polyester or aliphatic-aromatic co-polyesters. The majority of these biodegradable polymers are produced using a polycondensation method, and the raw materials are obtained from petrochemical feedstocks.[2] Unlike other petrochemical-based resins that take centuries to degrade after disposal, these polymers rapidly break down into carbon dioxide, water, and humus in appropriate conditions where they are exposed to the combined attack of water and microorganisms. These products meet advanced composting standards (like those found in UK, USA, and Japan), typically breaking down in twelve weeks under aerobic conditions.[2, 4]

One of the most interesting polymer in this direction is poly[(butylene succinate)-co-adipate] (PBSA). PBSA is a random co-polymer of poly(butylene succinate) (PBS) and adipate, and it is synthesized by polycondensation of 1,4-butanediol in the presence of succinic and adipic acids with relatively low production cost.[4, 5] PBSA, compared with PBS, is more susceptible to biodegradation because of its lower crystallinity and flexibility of polymer chains.[6] PBSA shows a number of interesting physical properties, including biodegradability; melt processability and chemical resistance. Because of its environmentally-friendly feature, it has been used as a degradable plastic for uses in service-ware, grocery and waste-composting bags, and mulch-films.[2, 7] However, inherent mechanical, barrier to gas and water-vapor, and melt-state viscosity of PBSA are not sufficient enough for wide-range of applications. With this in mind, over the last few years, attempts have been

*Author to whom correspondence should be addressed.

made to improve the properties of neat PBSA in order to make it more competitive with the conventional non-biodegradable polymers such as low density polyethylene. One such way of improving properties of these biopolymers is through the clay-containing polymer nanocomposite technology.[2, 8–20]

Lim et al.[21] first reported the preparation of biodegradable aliphatic polyester (Skygreen 2109) (BAP)/montmorillonite (MMT) nanocomposites, characterized them and studied thermal and rheological properties. The BAP were copolymers synthesized from diols (1,4 butanediol and ethylene glycol) and dicarboxylic acids (succinic and adipic). They dissolved different amounts of BAP into chloroform whereas; C25A (Closite®25A) organoclay was also dispersed in chloroform for 48 h. The chloroform from a mixture of both was then evaporated and the samples dried in vacuum for 24 h. These nanocomposites largely formed intercalated structures.

In recent years, Ray and various co-workers[4, 22] have prepared PBSA-clay nanocomposites through melt intercalation technique. Their studies began by testing clays with different extents of hydrophobicity, and hence different levels of interaction between the surfactants with the polymer matrix. In a typical experiment, three OMMTs were used: C15A; C93A (Closite®93A); and C30B (Closite®30B) and different composite structures obtained: phase-separated; intercalated; and a coexistence of intercalated and exfoliated, depending on the polarity of the surfactants used to modify the MMT. A higher degree of dispersion of the C30B clay was attributed to more favorable enthalpic interactions between the diols present in the C30B surfactant and the C=O groups present on the PBSA backbone. Hence, PBSA/C30B nanocomposite showed relatively better improvement in properties.

Chen and Yoon[23] used melt intercalation method to produce PBSA/C25A nanocomposites. In their work, the C25A was twice-functionalized with two types of silane coupling agents: (glycidyloxypropyl)trimethoxy silane and (methacryloyloxypropyl)trimethoxy silane. They observed stacks of clay layers well-dispersed in the PBSA matrix with multiple ordered platelets. The higher degree of exfoliation of the silicate layers in the case of twice-functionalised organoclay as compared to C25A was attributed to two factors: the reaction between the end-groups of PBSA and the epoxy groups on the coupling agents; and the polar interaction between the ester groups in the coupling agents and PBSA.

This article reports the preparation of multifunctional PBSA/organically modified synthetic fluorine mica (OSFM) nanocomposites. Like MMT, SFM also belongs to the same generally family of 2:1 layered or phyllosilicates. The only difference between MMT and SFM is that SFM ($NaMg_{2.5}(Si_4O_{10})F_2$) contains 'F' groups on its surface and it has much higher aspect ratio (length of each platelet ~200–300 nm) than that of MMT. The PBSA nanocomposite with 6 wt.% OSFM loading was prepared via melt-mixing technique. The structure and morphology of obtained nanocomposite was evaluated using X-ray diffraction (XRD) and transmission electron microscope (TEM). The mechanical and material properties of neat PBSA and its OSFM nanocomposites are also reported.

2. EXPERIMENTAL DETAILS

2.1. Materials

The OSFM used in this study was supplied by CO-OP Chemicals Ltd., Japan, and was synthesized by replacing Na^+ in SFM (original thickness of ~1 nm) of a cation exchange capacity (*CEC*) of 120 mequiv/100 g with *N*-(coco alkyl)-*N*,*N*-[bis(2-hydroxyethyl)]-*N*-methylammonium cation by ion exchange reaction. The reason for choosing *N*-(coco alkyl)-*N*,*N*-[bis(2-hydroxyethyl)]-*N*-methylammonium modified SFM as an clay in this study is due to the closest value of solubility parameter of the surfactant with that of PBSA. The solubility parameter (δ) for PBSA and organic modifier, *N*-(coco alkyl)-*N*,*N*-[bis(2-hydroxyethyl)]-*N*-methylammonium was roughly calculated from the group contribution methods of Fedors.[24] The values of δ for PBSA and surfactant are 23.8 and 22.5 $J^{1/2} \cdot cm^{-3/2}$, respectively.

The PBSA used in this study is a commercial product from Showa High Polymer (Japan), with the designation BIONOLLE #3001, which according to the supplier has a weight average molecular weight, $M_w = 190$ kg/mol, density = 1.23 g/cm^3 (ASTMD729), melt flow index (MFI) = 1.8 gm/10 min (190 °C, ASTM1238), glass transition temperature, $T_g = -43.8$ °C, and melting temperatures, T_m's = 83.1 °C (first) and 94.5 °C (second). The molar ratio of succinate unit to the adipate unit is ~4:1 and the content of the coupling agent (hexamethylene diisocyanate) unit is ~0.5 mol%.

2.2. Nanocomposite Processing

The PBSA nanocomposites containing 6 wt.% OSFM was prepared through melt-mixing using a twin rotor thermohaake-mixer (Polylab system) operated at 135 °C (set point) and a rotor speed of 60 rpm for 8 min. OSFM powder was slowly added after two and half minutes of melting of PBSA inside the mixer, which was considered as time zero. The obtained nanocomposite strands were then dried under vacuum at 65 °C for 7 h to remove any residual water. The dried nanocomposite sample was molded using a Carver laboratory press at 2 MPa at 135 °C for 15 min.

2.3. Characterization and Property Measurements

The best-known technique to study the dispersion of clay platelets in polymer matrices is powder XRD. Compression molded samples were analyzed in an X'Pert PRO diffractometer (PANalytical, the Netherland) in reflection

mode. The operating voltage and current were 45 kV and 40 mA, respectively. The wavelength of the Ni-filtered Cu K_α radiation was 0.1542 nm. The exposure time and scan speed for XRD measurements were 19.7 min and 0.036987 °/s, respectively.

The clay platelets in the polymer matrix were directly visualized using high-resolution transmission electron microscopy (HRTEM), which was carried out for both extruded and compression molded samples. Sections (70–80 nm) from all samples were obtained with a Leica (Austria) EM FC6 cryo-ultramicrotome set at −120 °C and at a cutting speed of 0.07 mm/s using a Diatome 35° diamond knife (Diatome, Switzerland). HRTEM images of pristine platelets were obtained by dispersing clay powder in ethanol, and mounting on carbon-coated grids after 30 s untrasonication. Calibrated images were captured with JEOL2100 HRTEM (JEOL, Japan) set at an operating voltage of 200 kV and using a Gatan Ultrascan camera and Digital Micrograph software.

DMA was performed using a PerkinElmer DMA8000 analyzer in the dual cantilever bending mode. The temperature dependence of the storage modulus (E') was measured at a frequency of 1 Hz. The strain amplitude was 0.05% and the heating rate was 2 °C/min from −100 to 80 °C. The glass transition temperature (T_g) of various samples was measured from the deflection point in the E' curves.

Tensile testing was performed using an Instron 5966 tester (Instron Engineering Corporation, USA) with a load cell of 10 kN, and the tensile properties including, modulus and yield strength were determined. The test was performed under tension mode at a single strain rate of 50 mm/min at ambient temperature (25 °C) and 50% relative humidity. The strain was measured by the displacement of the crosshead. Specimens were approximately 2.1 mm-thick dog bone plate prepared through compression molding. The results presented are an average of six independent measurements.

Oxygen gas (OTR) transmission rates of neat PCL and various composite samples were measured with a MOCON OX-TRAN® Model2/21 from Modern controls Inc, Minneapolis, USA, respectively. Aluminum masks were used to reduce the film test area to 5 cm^2. The temperature was fixed at 23 °C for OTR; relative humidity (RH) was 50% during measurements. Samples were pretreated for 24 h at experimental conditions prior to the test. During the pretreatment period, film samples were placed between the two halves of the permeability cell and flushed with a carrier gas to remove trace oxygen from the cells and films. Oxygen gas was introduced to one surface of the sample at atmospheric pressure. The samples were run until steady-state conditions were reached, and the OTR was recorded from the systems. Film thicknesses were measured using digital calipers; averages of eight different positions were calculated and the mean was used.

Thermogravimetric analyses (TGA) were conducted on a TG-Q500 (TA Instruments) analyzer. Samples weighing approximately 11 mg were heated from room temperature to 900 °C at a heating rate of 10 °C/min under air atmosphere. To obtain characteristic thermal stability indicators such as the onset degradation temperature, three independent tests were carried out per sample, and the average value was reported.

3. RESULTS AND DISCUSSION

The nanocomposite structure is generally characterized by XRD pattern and TEM observation. Direct evidence of the intercalation of the polymer chain into the silicate galleries is provided by XRD patterns in the range of $2\theta = 1$–$10°$. Figure 1 shows the result of XRD patterns of pure OSFM powder and corresponding nanocomposite prepared with 6 wt.% of OSFM. The characteristic mean interlayer spacing of the (001) plane ($d_{(001)}$) for the OSFM powder is 2.06 nm ($2\theta = 4.29°$). In the XRD pattern of nanocomposite, the intensity of the characteristic peak of OSFM was significantly reduced and a broad peak was observed at $2\theta = 2.82°$ ($d_{(001)} = 3.13$ nm), indicating that the structure is potentially highly intercalated, due to the possible favorable interaction between the 'CO' group on the PBSA backbone with the diols present in the surfactant used for the modification of SFM.

To support XRD pattern, TEM observation was used to directly and qualitatively visualize the state of silicate layers dispersion/exfoliation in the PBSA matrix. Figure 1 (inset) also shows the TEM bright field image of nanocomposite corresponding to the XRD pattern, in which dark entities are the cross section of intercalated OSFM layers. TEM image for nanocomposite reveals that there are

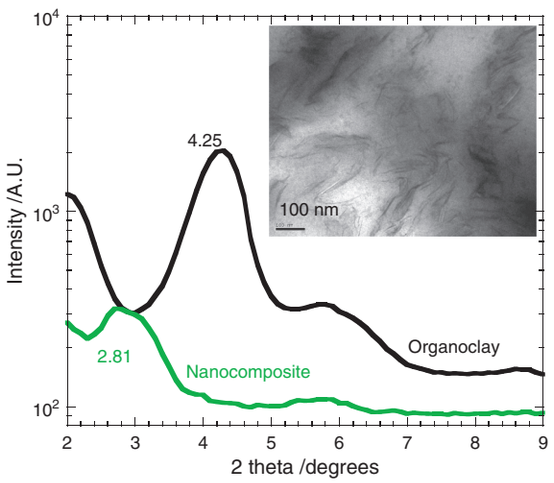

Figure 1. X-ray diffraction patterns of pure organically modified synthetic fluorine mica and poly[(butylene succinate)-co-adipate] nanocomposite. Inset showing the bright filed transmission electron microscopy image of nanocomposite in which black entities are dispersed silicate layers.

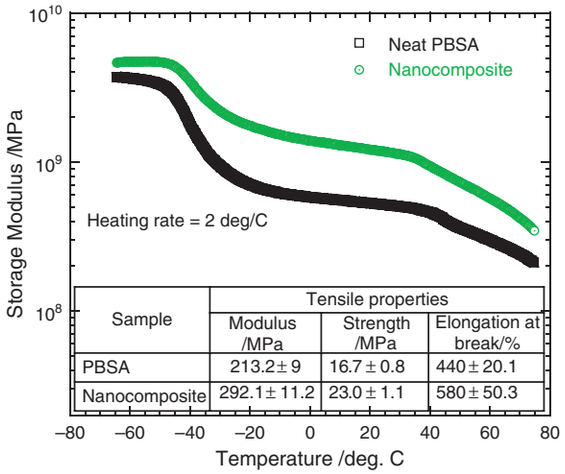

Sample	Tensile properties		
	Modulus /MPa	Strength /MPa	Elongation at break/%
PBSA	213.2± 9	16.7 ± 0.8	440 ± 20.1
Nanocomposite	292.1± 11.2	23.0 ± 1.1	580 ± 50.3

Figure 2. Temperature dependence storage modulus of neat poly[(butylene succinate)-co-adipate] and its nanocomposite with organically modified synthetic mica. Inset table summarized the tensile properties.

some intercalated stacked and disordered and/or exfoliated silicate-layers coexisting in the nanocomposites. The stacked and intercalated silicate layers are responsible for weak XRD diffractions as observed in XRD patter whereas the disordered and exfoliated silicate layers have no periodic stacking and thus remain XRD silent.[25] This kind of mixed intercalated and/or exfoliated structure originates from the chemical and size inhomogeneities of the silicate layers. Typically the larger-in lateral size-silicate layers create stacked intercalated structure, whereas the smaller layers tend to exfoliate.[26]

Figure 2 shows the temperature dependence storage modulus of neat PBSA and its OSFM-containing nanocomposite. It can be seen from the figure, over the all experimental temperature range, the storage modulus of neat PBSA was significantly improved after nanocomposite formation with 6 wt.% OSFM. At room temperature (25 °C), the extent of increase in modulus of nanocomposite is 140% compared to that of neat PBSA. It is interesting to note that the matrix glass transition temperature was not affected after incorporation of OSFM, but nanocomposite showed significant improvement in modulus over the entire temperature range. Such an observation may be related to the high degree of intercalation of polymer chains into the OSFM silicate layers of the OSFM, which leads to the large surface area for the favorable interactions between silicate layers and the polymer matrix. Polymer chains inside the silicate galleries are immobilized and the effect of immobilization on the polymers chains may be the main responsible factor for this substantial increase in storage modulus. The similar type of behavior was also observed in the case of PBSA/C30B nanocomposite[27] but the level of improvement is higher in the case of PBSA/OSFM nanocomposite with respect to PBSA/C30B nanocomposite containing the same amount of organoclay loading. We believe higher aspect ratio of SFM platelets is responsible for such observation.

The tensile properties of compression molded samples of neat PBSA and its nanocomposite are reported as inset in Figure 2. Prior to measurement, samples were annealed for 60 °C under vacuum for overnight and an average of eight tests is presented here. It is clear from the figure that tensile properties of PBSA were concurrently improved after nanocomposite formation with OSFM. This is quite unusual observation in the case of polymer/clay nanocomposites but we believe high degree of intercalation of PBSA chains into OSFM leads to the higher degree of delamination of SFM platelets in PBSA matrix. Therefore, the active surface area of the dispersed silicate platelets increased tremendously, results very efficient stress transfer between the matrix and silicate platelets. Another reason may be due to the degree of overall crystallinity of PBSA matrix after nanocomposite formation. Kojima et al.[28] explained improved toughness of nylon 6/clay nanocomposites on the basis of decrease degree of crystallinity of matrix after nanocomposite formation.

Nanoclay platelets are believed to be able to reduce the gas permeability of polymer matrices through the formation of a tortuous path through the filler layers, which retards the diffusion and passage of the gas molecules through the matrix.[29] The barrier properties of composites based on nanoclays are affected by a number of factors, such as the volume fraction of the nanoclays, the aspect ratio of the clays, the extent of the dispersion of the clays, the orientation of the clays within the matrix and the polymer-chain-confinement effects that arise as a result of intercalation.

The oxygen gas permeability of neat PBSA (87 ml · mm/m^2 · day · MPa) was significantly reduced after nanocomposite (22 ml · mm/m^2 · day · MPa) formation with OSFM. This improved is much higher than the PBSA

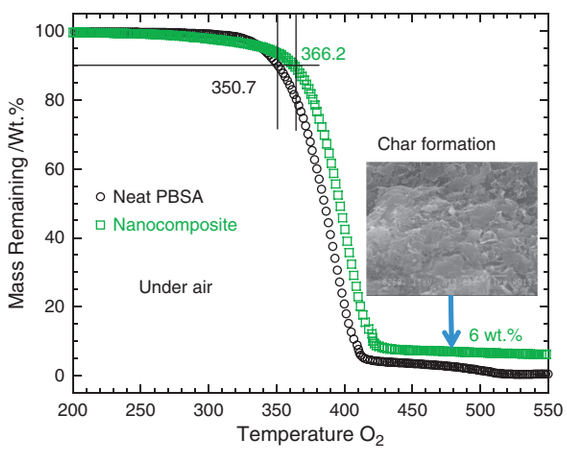

Figure 3. Thermogravimetric traces of neat poly[(butylene succinate)-co-adipate] and it nanocomposite with organically modified synthetic fluorine mica under air environment. Inset shows the scanning electron microscopic image of char formation.

nanocomposite prepared with the same amount of C30B. The difference in the barrier properties has been attributed to the difference in the aspect ratios of the two clay types. SFM clay has larger lateral dimensions than the MMT, and therefore, for equal volume loading and assuming near similar dispersion, the SFM would hinder the flow of the oxygen molecules more than the MMT.[29]

Another important property improvement for nanocomposite is overall thermal stability. In Figure 3 we present typical TGA traces of weight loss of neat PBSA and its nanocomposite as a function of temperature under thermo-oxidative environment. In the TGA thermgram of nanocomposite, a small weight loss (around 2.45%) was observed in the temperature range of 225 to 335 °C. This may be due to the degradation of surfactant used to modify SFM. The thermal stability of the samples was determined by ascertaining the onset degradation temperature, which is the temperature after a weight loss of 10%, T_{10}. In the case of nanocomposite, with the addition of 6 wt.% OSFM, there was a 16.2 degree increased in T_{10}. Moreover, the overall thermal stability and char formation were much higher in the case of nanocomposite when compared with respect to the neat PBSA. Such observations indicate efficient flame retardant property of OSFM. This improved thermal stability in the case of nanocomposite is due to the presence of highly dispersed intercalated silicate layers in PBSA matrix.

4. CONCLUSIONS

The nanocomposite of biodegradable PBSA and OSFM was prepared using melt-blending. The structure and morphological studied using XRD and TEM revealed the homogeneous dispersion of intercalated silicate layers in PBSA matrix. Various properties such as mechanical, barrier, thermal stability, etc. were measured and results showed that the inherent properties of neat PBSA were concurrently improved after nanocomposite formation with OSFM. Therefore, the obtained nanocomposite has multiple functional properties including biodegradability and finds application in packaging industry.

Acknowledgment: The authors (Shaeel A. Al-Thabaiti, Suprakas Sinha Ray, Sulaiman Nassir Basahel, and Mohamed Mokhtar) would like to thank the Deanship of Scientific Research (DSR), King Abdulaziz University, Jeddah, for financial support (under grant number MG/33/8).

References and Notes

1. V. Ojijo and S. S. Ray, *Prog. Polym. Sci.* 38, 1543 **(2013)**.
2. S. S. Ray, Environmentally Friendly Polymer Nanocomposites: Types, Processing and Properties, Woodhead Publishing, London **(2013)**.
3. S. S. Ray, *Acc. Chem. Res.* 45, 1710 **(2012)**.
4. V. Ojijo and S. S. Ray, Environmental Silicate Nano-Biocomposites, edited by L. Avérous and E. Pollet, Springer, London **(2012)**, Chap. 7.
5. D. R. Ishioka, E. Kitakuni, and Y. Ichikawa, Aliphatic Polyesters: 'Bionolle,' edited by Y. Doi and A. Steinbuchel, Biopolymers, Polyesters III, Application and Commercial Products, Weinheim, Wiley-VCH Verlag Gmbh **(2002)**, Vol. 4. p. 275.
6. M. S. Nikolic and J. Djonlagic, *Polym. Degrad. Stab.* 74, 263 **(2001)**.
7. T. Fujimaki, *Polym. Degrad. Stab.* 59, 209 **(1998)**.
8. S. S. Ray, Clay-containing polymer nanocomposites, From Fundamental to Real Applications, Elsevier, Amsterdam **(2013)**.
9. M. Naffakh, C. Marco, M. A. Gómez, G. Ellis, W. K. Maser, A. Benito, and M. T. Martínez, *J. Nanosci. Nanotechnol.* 9, 6120 **(2009)**.
10. Y. S. Yun, H.-R. Pyo, J. Y. Lee, I.-J. Chin, and H.-J. Jin. *J. Nanosci. Nanotechnol.* 13, 7062 **(2013)**.
11. X. Li, Y. Liu, D. Li, and Y. Huang, *J. Nanosci. Nanotechnol.* 13, 5924 **(2013)**.
12. P.-C. Chiu, R. Y.-T. Su, J.-Y. Yeh, C.-Y. Yeh, and R. C.-C. Tsiang, *J. Nanosci. Nanotechnol.* 13, 3910 **(2013)**.
13. G. Kim, S. Kim, S.-Y. Lee, M. Hussain, and Y.-H. Choa, *J. Nanosci. Nanotechnol.* 13, 3936 **(2013)**.
14. J. Lee, Y. S. Yun, D. H. Kim, H. H. Park, and H.-J. Jin, *J. Nanosci. Nanotechnol.* 13, 1769 **(2013)**.
15. M. R. de Moura, F. A. Aouada, L. H. C. Mattoso, and V. Zucolotto, *J. Nanosci. Nanotechnol.* 13, 1946 **(2013)**.
16. Y. Chen, W. Xu, Y. Xiong, C. Peng, W. Liu, G. Zeng, and Y. Peng, *J. Nanosci. Nanotechnol.* 13, 2136 **(2013)**.
17. H. Wang and X. Lai, *J. Nanosci. Nanotechnol.* 13, 1511 **(2013)**.
18. W.-De. Zhang, Y.-M. Zheng, Y.-S. Xu, Y.-X. Yu, Q.-S. Shi, L. Liu, H. Peng, and Y. Ouyang, *J. Nanosci. Nanotechnol.* 13, 409 **(2013)**.
19. H.-J. Kim, Y. Kwon, and C. K. Kim, *J. Nanosci. Nanotechnol.* 13, 577 **(2013)**.
20. L. G. Bach, Md. R. Islam, Y. H. Kim, S. D. Seo, C. Park, H. G. Kim, and K. T. Lim, *J. Nanosci. Nanotechnol.* 13, 694 **(2013)**.
21. S. T. Lim, Y. H. Hyun, and H. J. Choi, *Chem. Mater.* 14, 1839 **(2002)**.
22. S. S. Ray and V. Ojijo, *Prog. Mater. Sci.* submitted **(2013)**.
23. G. Chen and J.-S. Yoon, *Polym. Inter.* 54, 939 **(2005)**.
24. D. W. V. Krevelen, Properties of Polymer, Amsterdam, Elsevier, The Netherlands **(1990)**.
25. V. A. Dritis, X-Ray Diffraction by Disordered Lamellar Structures, Springer, New York **(1990)**, p. 21.
26. S. S. Ray, K. Yamada, M. Okamoto, A. Ogami, and K. Ueda, *Chem. Mater.* 15, 1456 **(2003)**.
27. S. Sinha Ray and M. Bousmina, *Macromol. Mater. Eng.* 290, 759 **(2005)**.
28. Y. Kojima, A. Usuki, M. Kawasumi, A. Okada, Y. Fukushima, T. Kurauchi, and O. Kamigaito, *J. Mater. Res.* 8, 1185 **(1993)**.
29. S. S. Ray, K. Yamada, M. Okamoto, and K. Ueda, *Nano Lett.* 2, 1093 **(2002)**.

Received: 23 March 2013. Accepted: 16 December 2013.